J. Meas. Sci. Instrum., 2026, 17(1): 88-96.
DOI: 10.62756/jmsi.1674-8042.2026007
http://jmsi.publish.founderss.cn
jmsi@nuc.edu.cn

# A dehazing algorithm of compensated transmission based on negative haze concentration correction

LÜ Dongxia, YANG Yan*

*School of Electronics and Information Engineering, Lanzhou Jiaotong University, Lanzhou 730070, China*

***Corresponding author:** YANG Yan (yangyantd@mail.lzjtu.cn)

**Received:** December 26, 2024 **Revised:** April 19, 2025 **Accepted:** September 10, 2025

**Abstract:** Aiming at the problems such as halos, artifacts and incomplete dehazing in hazy image restoring processing, a dehazing algorithm of compensated transmission based on negative haze concentration correction is proposed. First of all, the error mechanism is used to compensate for the transmission of the dark channel prior (DCP), observing the relationships among transmission, depth of field, and haze concentration. A negative haze concentration model is constructed to adaptively correct the transmission of gamma in this study. Finally, the channel difference fusion-based median channel is proposed to correct local atmospheric veil and combined with the atmospheric scattering model to recover haze-free image. The experimental results show that the algorithm solves the problems of halos, artifacts and incomplete dehazing with outstanding details and appropriate brightness.

**Key words:** image dehazing; compensated transmission; negative haze concentration; channel difference; local atmospheric light

## 0 Introduction

In harsh environments such as haze, there are a large number of suspended particles in the air, and light is absorbed and scattered by these particles, making images acquired by imaging devices severely degraded[1], specifically in terms of color shift, contrast reduction, loss of details, and local brightening, which reduces the utilization rate of the information value carried by images. Therefore, it is of major research significance to restore images acquired in hazy weather. Currently, there are two main types of methods for clarification of hazy images: traditional methods and deep learning-based methods.

Traditional methods include image enhancement and physical model-based image restoration. Image enhancement methods[2-4] include histogram equalization, Retinex algorithm, wavelet transform[5], etc. This family of algorithms achieve the purpose of image restoration by selectively highlighting the features of interest in the hazy image by certain means. However, these algorithms do not consider the degenerate mechanism of the image, so there is some information loss in enhancement results, and dehazing effect is not ideal. Image restoration based on physical models uses image degenerate mechanism to develop the degradation process, establishes mathematical models to estimate unknown parameters through priors or assumptions, and finally achieves image restoration. In recent years, image restoration methods based on physical models have developed rapidly. He et al.[6] proposed dark channel prior (DCP) dehazing algorithm through the observation of a large number of clear images. Agrawal et al.[7] presented super-pixel and nonlinear transformation dehazing algorithm. Zhu et al.[8] comed up with color attenuation prior (CAP). Yang et al.[9] proposed edging-preserving function instead of the minimum filter fitting dark channel dehazing algorithm. Yang et al.[10] proffered composite channel prior (CCP) to achieve an accurate estimation of transmission. Since restoration of hazy images based on physical models requires priors and assumptions for the aided calculation of transmission and related parameters, it can obtain more realistic dehazed images because it takes into account the cause of hazy images.

Deep learning-based image dehazing algorithms need to train a great number of samples to obtain model parameters and build a network to achieve image dehazing. A multi-scale convolutional neural network (MSCNN) for transmission estimation was designed by Ren et al.[11]. The main idea is to fuse the transmission obtained from coarse-scale network with that from fine-scale network to achieve better recovery results. Li et al.[12] integrated transmission and atmospheric light into a covariate, and designed a

© The Author(s) 2026. Published by Publishing Center of North University of China. The articles published in this open access journal are distributed under the terms of the Creative Commons Attribution 4.0 International License (http://creativecommons.org/licenses/by/4.0/), which permits use, distribution and reproduction in any medium, provided the original work is properly cited.

lightweight multi-scale network structure, all-in-one dehaze network (AOD-Net), which eliminates the errors of training atmospheric light and transmission separately and achieves better recovery results. However, the algorithm has the problem of incomplete dehazing and overall dark recovery results. An end-to-end feature fusion attention network (FFA-Net) was proposed by Qin et al.[13], which can effectively extract image features and recover haze-free images directly, but the network structure is overfitting and the recovery effect is not satisfactory for real scene-hazed images. Self-guided image dehazing using progressive feature fusion was introduced by Bai et al.[14], which can explore useful information from the input hazy image itself as a guide to help image dehazing. However, the method cannot process blurred images containing light sources and does not support multiple manual processing, therefore, it is not used as the mist model. In recent years, this type of methods have been used more often, but the dataset trained by them consists of synthetic images, which does not take into account the nature of image degradation, making the processing of hazy images in real environments less effective. Additionally, the use of a large number of convolutional operations in the network leads to high computational complexity, requiring a high-configuration experimental environment.

Aiming at the shortcomings of the above researches, we propose a dehazing algorithm of compensated transmission based on negative haze concentration correction. Firstly, the transmission of the dark channel is compensated, and negative haze concentration is used to adaptively correct the dark channel transmission to acquire accurate transmission. Then, the initial local atmospheric light is obtained through channel difference and morphological operation, and the local atmospheric light is obtained by cross-bilateral filtering of the initial atmospheric light. Finally, the image is restored through the atmospheric scattering model. Experimental results show that the color restored by the proposed algorithm is natural, the texture details are rich, and the dehazing effect is remarkable.

# 1 Related work

## 1.1 Atmospheric scattering model

In the field of computer vision, the formation of a hazy image is usually represented by atmospheric scattering model, which can be expressed as

$$I(x,y)=J(x,y)t(x,y)+A(1-t(x,y)), \quad (1)$$

where $(x,y)$ is the pixel position, $I(x,y)$ is the degraded scene, $J(x,y)$ is the recovered scene, $t(x,y)$ is the medium transmission, and $A$ is the atmospheric light. In the homogeneous medium, transmission is related to the scene depth as

$$t(x)=\mathrm{e}^{-\beta d(x)}, \quad (2)$$

where $\beta$ is the atmospheric scattering coefficient, and $d(x)$ is the scene depth. According to the atmospheric scattering model, if the atmospheric light and transmission are known, the haze-free image can be recovered.

## 1.2 DCP theory

Starting from an atmospheric scattering model, based on a large number of experimental statistics, He et al.[6] obtained outdoor haze-free images with very small pixel values and converging to 0 in at least one color channel for large non-sky and high brightness regions, proposing the dark channel prior (DCP) theory expressed as

$$J^{\mathrm{dark}}(x,y)=\min_{x,y\in\alpha}\left(\min_{c\in(\mathrm{r,g,b})}(J^c(x,y))\right)\to 0, \quad (3)$$

where $J^{\mathrm{dark}}(x,y)$ is the dark channel of the haze-free image, $\alpha$ is the neighborhood centered on the pixel point, $J^c$ denotes the r, g, and b color channels of the image. The transmission can be obtained by applying the minimum filtering operation on both sides of Eq. (1) and combining it with Eq. (3), namely

$$t_1(x,y)=1-\min_{x,y\in\alpha}\left(\min_{c\in(\mathrm{r,g,b})}\left(\frac{I^c(x,y)}{A}\right)\right). \quad (4)$$

In order to make the image clearer and more natural, the coefficient $\omega$ is introduced, and its empirical value is 0.95. Then, we can get

$$t_2(x,y)=1-\omega\min_{x,y\in\alpha}\left(\min_{c\in(\mathrm{r,g,b})}\left(\frac{I^c(x,y)}{A}\right)\right). \quad (5)$$

According to Eq. (1), the haze-free image can be obtained as

$$J(x,y)=\frac{I(x,y)-A}{\max(t_2(x,y),t_0)}+A. \quad (6)$$

The shortcomings of DCP restoration results are as follows: the restored image has block effects, and the sky area has false color and color cast. The reasons for this deficiency are: 1) the minimum filtering is used twice when processing the transmission, which makes the information near the edge of the image missing, leading to over-estimation of the transmission. 2) DCP fails in large bright sky regions, resulting in an under-estimation of the transmission in these regions. As shown in Fig. 1, the blocky effect at the edges, the pseudo-color in the sky, and the halo effects appear in the haze-free image recovered by DCP.

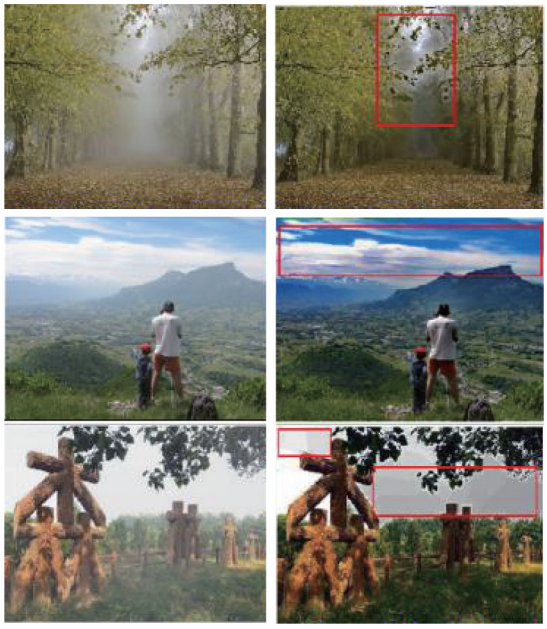


**Fig. 1 Restored images by DCP. (a) Hazy images, and (b) Restored images by DCP**

## 2 Proposed algorithm

According to the atmospheric scattering model, accurate estimation of transmission and atmospheric light is essential for obtaining haze-free images. Based on DCP theory, we propose a dehazing algorithm that can estimate the transmission and atmospheric light accurately.

Firstly, the error mechanism is used to compensate for the transmission of the dark channel prior, observing the relationships among transmission, depth of field, and haze concentration. Secondly, a negative haze concentration model is constructed, with adaptive gamma correction to obtain the transmission. Finally, the channel difference fusion-based median channel is proposed to correct local atmospheric light, and then combined with the atmospheric scattering model to recover the haze-free image.

The flowchart of our method is shown in Fig.2.

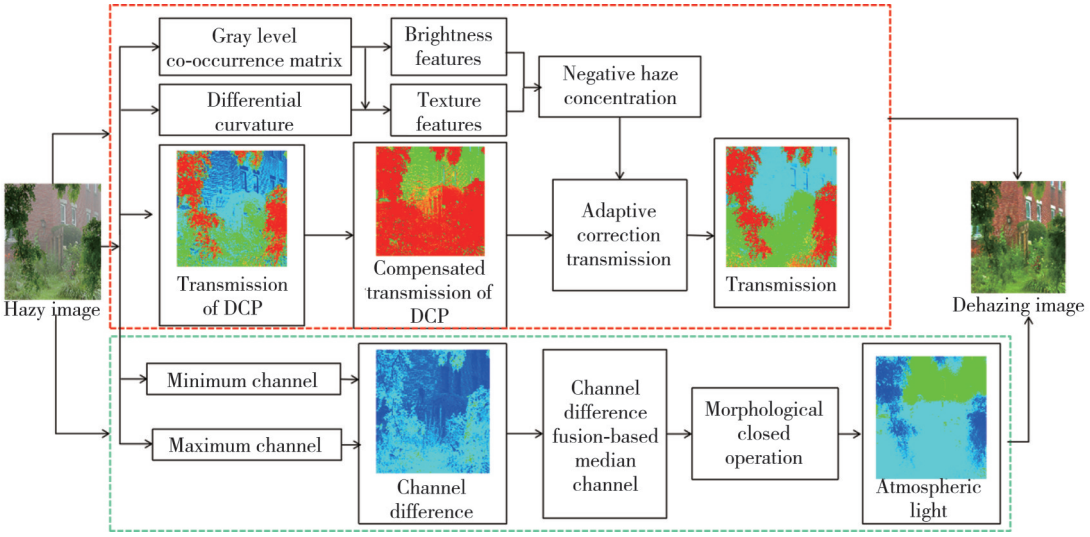


**Fig. 2 Flowchart of proposed algorithm**

### 2.1 Compensated transmission

Since the transmission estimated by DCP is too small in the sky region and too large in the edge region, the transmission obtained by DCP needs to be compensated. When $J^{\text{dark}}(x,y)$ is not 0, the expression of the transmission is

$$t_3(x,y)=\frac{A-\min\limits_{c\in(\text{r,g,b})}\left(I^c(x,y)\right)}{A-\min\limits_{c\in(\text{r,g,b})}\left(J^c(x,y)\right)}, \tag{7}$$

According to Eqs. (5) — (7), it is clear that there is an error in the transmission estimated by DCP, so the error mechanism is described as

$$\theta=t_3(x,y)-t_2(x,y), \tag{8}$$

where $\theta$ is the transmission error following Gaussian distribution, which is to compensate for the transmission of the dark channel. The compensated transmission can be obtained as

$$t(x,y)=t_1(x,y)+\frac{1}{\sqrt{2\pi}\,\sigma}\mathrm{e}^{-\frac{\min\limits_{c\in(\text{r,g,b})}\left(I^c(x,y)\right)}{2\sigma^2}}. \tag{9}$$

### 2.2 Adaptive correction to compensate for transmission

After being compensated, the transmission is deviated in some areas.

In order to obtain accurate transmission, gamma correction is proposed as

$$t(x,y)=t_1(x,y)+\left(\frac{1}{\sqrt{2\pi}\,\sigma}\mathrm{e}^{-\frac{\min\limits_{c\in(\mathrm{r,g,b})}(I^c(x,y))}{2\sigma^2}}\right)^{\gamma}. \quad (10)$$

For different hazy images, the values of $\gamma$ are taken differently, so the compensated transmission can be adaptively corrected according to Refs.[8, 15-17]. Then, we can get

$$d(x,y)\propto c(x,y)=l(x,y)-q(x,y), \quad (11)$$

where $c(x,y)$ is the haze concentration, $l(x,y)$ is the luminance characteristics, and $q(x,y)$ is the texture feature. According to Eqs. (2) and (11), it can be seen that transmission is negatively correlated with scene depth, scene depth is positively correlated with haze concentration, haze concentration is positively correlated with luminance characteristics, and haze concentration is negatively correlated with texture features. Therefore, the transmission is negatively correlated with the haze concentration, and the adaptive gamma correction is

$$\gamma=-c(x,y)=-(l(x,y)-q(x,y)), \quad (12)$$

the gray level co-occurrence matrix is utilized to extract the luminance characteristics $c(x,y)$ and coarse-level texture feature $q_1(x,y)$ of the image. Because the gray level co-occurrence matrix does not take into account the local changes of the image, this term is combined with differential curvature to better represent texture feature.

$$\begin{cases} a=\dfrac{\left(\dfrac{\partial I(x,y)}{\partial x}\right)^2\dfrac{\partial^2 I(x,y)}{\partial x^2}+2\dfrac{\partial I(x,y)}{\partial x}\dfrac{\partial I(x,y)}{\partial y}\dfrac{\partial^2 I(x,y)}{\partial xy}+\left(\dfrac{\partial I(x,y)}{\partial y}\right)^2\dfrac{\partial^2 I(x,y)}{\partial y^2}}{\left(\dfrac{\partial I(x,y)}{\partial x}\right)^2+\left(\dfrac{\partial I(x,y)}{\partial y}\right)^2}, \\ b=\dfrac{\left(\dfrac{\partial I(x,y)}{\partial y}\right)^2\dfrac{\partial^2 I(x,y)}{\partial x^2}-2\dfrac{\partial I(x,y)}{\partial x}\dfrac{\partial I(x,y)}{\partial y}\dfrac{\partial^2 I(x,y)}{\partial xy}+\left(\dfrac{\partial I(x,y)}{\partial x}\right)^2\dfrac{\partial^2 I(x,y)}{\partial y^2}}{\left(\dfrac{\partial I(x,y)}{\partial x}\right)^2+\left(\dfrac{\partial I(x,y)}{\partial y}\right)^2}, \end{cases} \quad (13)$$

$$q_2(x,y)=\|a|-|b\|, \quad (14)$$

$$q(x,y)=\frac{q_1(x,y)+q_2(x,y)}{2}, \quad (15)$$

where $a$ is the second derivative in the direction perpendicular to the gradient, $b$ is the second derivative in the direction of the gradient direction, and $q(x,y)$ is the result of bilateral filtering.

To verify the correctness of haze concentration extraction, real scenes and test set scenes are selected. As shown in Fig. 3(b), the haze concentration is larger in the area with the larger depth of field and smaller in the close range. From the three groups of images, it can be seen that the detail texture is almost invisible in the regions with large haze concentrations.

After extracting haze concentration, the corrected transmission is obtained according to Eqs. (10) — (12), and then cross-bilateral filtering is performed on it as the final transmission.

To verify the accuracy of the transmission obtained, a hazy image in a real scene is selected for simulation. Moreover, we compare the results by DCP with ours. As shown in Fig.4, in the restored results containing sky regions, the restored images by DCP have phenomena such as color cast, halo, and artifact. In contrast, the proposed algorithm with compensated transmission overcomes these drawbacks and can achieve accurate transmission. Moreover, the restored results show that hazes are completely removed, the brightness is suitable, and the color is natural.

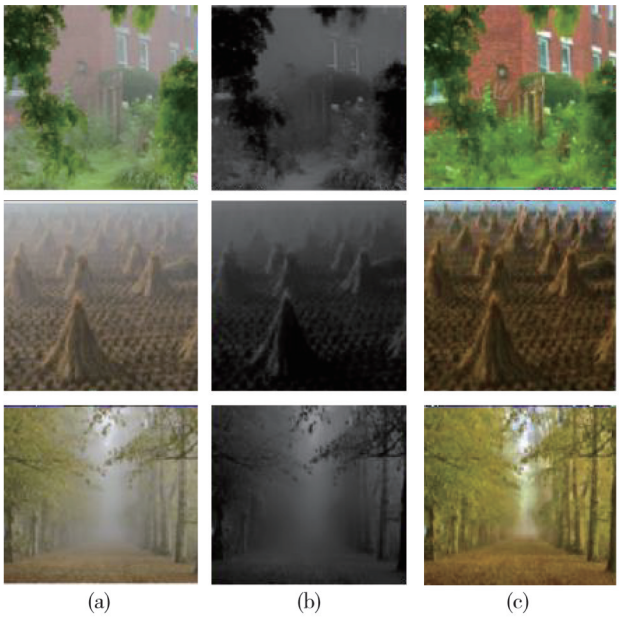


**Fig. 3 Hazy images and distributions of haze concentration. (a) Hazy images, (b) Distributions of haze concentration, and (c) Restored images by our method**

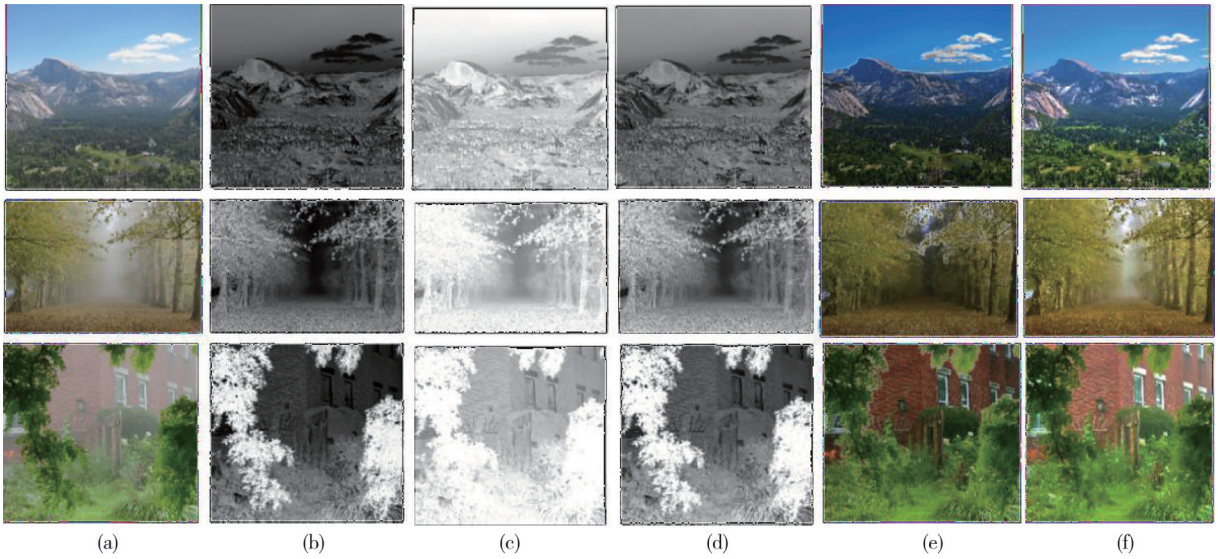


**Fig. 4 Comparison of transmittance and restoration results. (a) Hazy image, (b) Transmission of DCP, (c) Compensated transmission, (d) Corrected transmission, (e) Restored results by DCP, and (f) Restored images by our method**

## 2.3 Atmospheric light estimation

Atmospheric light is also a key parameter when restoring images based on the atmospheric scattering model. Its value may affect the brightness of dehazing images. If the estimation is too high, the restored image may be darker, and if the estimation is too low, the restored image may be brighter. Ref. [6] selects the average value of pixels corresponding to the top 0.1% of the brightest pixel points in the dark channel as the global atmospheric light value. This method is susceptible to bright objects, resulting in inaccurate estimation of atmospheric light value and unsatisfactory dehazing effects. Local atmospheric light is more accurate compared with global atmospheric light in low-luminance regions. Ref.[18] proposes a scheme to define the atmospheric light from the local region of the hazy image under the premise that the local light source in the scene is the same as the local atmospheric light. This method performs morphological operations and filtering on the maximum channel of the hazy image to obtain the local atmospheric light function, achieving a better dehazing effect. After statistics, it is found that there is a large difference between the maximum color channel and the minimum color channel for the general hazy image. The channel difference is shown in Fig.5(c).

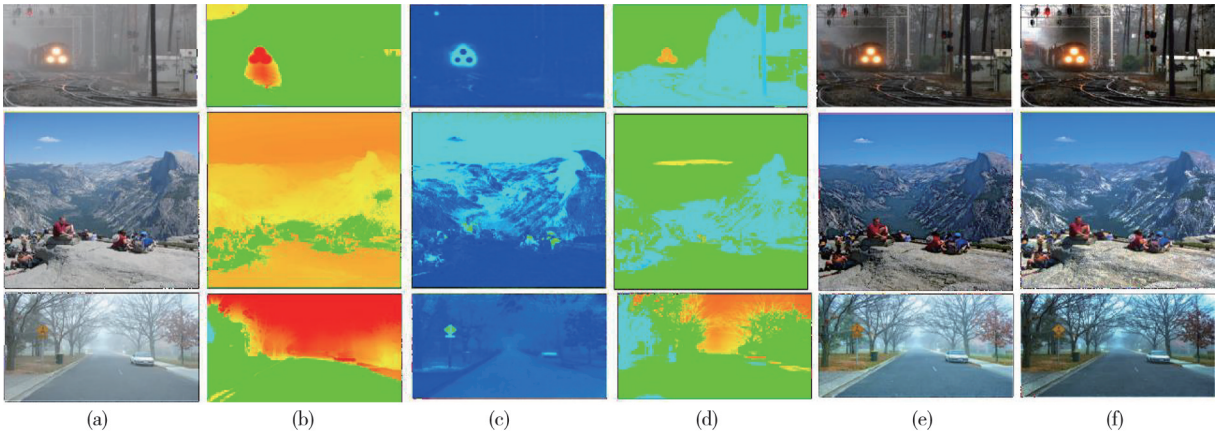


**Fig. 5 Comparison of atmospheric lights. (a) Hazy image, (b) Atmospheric light by Ref. [17], (c) Channel difference, (d) Atmospheric light by our method, (e) Restored images by Ref. [17], and (f) Restored images by our method**

Therefore, we propose a method of atmospheric light estimation fusing the channel difference[19-21] with the medium channel. First, the maximum and minimum channels of hazy images are extracted. Next, the medium channel is obtained by median filtering. Finally, the fusion process is shown as

$$\begin{cases} w_1(x,y)=\max\limits_{c\in(\mathrm{r,g,b})}(I^c(x,y)), \\ w_2(x,y)=\min\limits_{c\in(\mathrm{r,g,b})}(I^c(x,y)), \end{cases} \tag{16}$$

$$\begin{cases} m_1(x,y)=F(w_1(x,y)), \\ m_2(x,y)=F(w_2(x,y)), \end{cases} \tag{17}$$

$$\theta = w_1(x,y) - w_2(x,y), \tag{18}$$

$$A_1(x,y) = \theta m_1(x,y) + (1-\theta) m_2(x,y), \tag{19}$$

where $w_1(x,y)$ is the maximum channel, $w_2(x,y)$ is the minimum channel, $F(\bullet)$ is the median filter function, and $\theta$ is the channel difference. To remove the interference from some pixels, the morphological closed operation is performed on $A_1(x,y)$. After obtaining the estimation of atmospheric light, combining the transmission with Eq. (6), the hazy image is recovered. Overall, the local atmospheric light estimated by the proposed algorithm is better than that of Ref.[17], as shown in Fig.5.

## 3 Experimental results and analysis

In order to verify the feasibility and effectiveness of the proposed algorithm, a number of comparative experiments were conducted, and the restored results are compared from subjective and objective perspectives. The comparison algorithms include DCP method[6], non-linear transmission algorithm[7], haze removal algorithm[9], CCP method[10], FFA-Net[13], and self-guided image dehazing using progressive feature fusion[14].

### 3.1 Subjective evaluation

The subjective evaluation can directly show the difference between comparison algorithms from visual effect. This paper mainly presents the restoration effects of real degraded scenes and synthetic degraded scenes, the latter of which are selected from the open test set RESIDE. The restoration results of the first category without sky regions are shown in Fig.6, the restoration results of the second category with sky regions are shown in Fig.7, and the restoration results of the images from test set are shown in Fig.8.

(a)Hazy image (b) Ref.[6] (c) Ref.[7] (d) Ref.[9] (e) Ref.[13] (f) Ref.[14] (g) Ref.[10] (h) Our method

**Fig. 6 Restoration effects of hazy images without sky regions**

(a)Hazy image (b) Ref.[6] (c) Ref.[7] (d) Ref.[9] (e) Ref.[13] (f) Ref.[14] (g) Ref.[10] (h) Our method

**Fig. 7 Restoration effects of hazy images with sky regions**

As can be seen from Figs. 6 and 7 that the dehazing effects of DCP algorithm[6] are incomplete and colors are distorted. The algorithm of Ref. [7] has good color retention, but some of the images appear distorted. The dehazing effects of Ref.[10] are good, but the sky regions are not completely dehazed. Overall, our method achieves the desired effects with thorough dehazing and natural colors. It not only overcomes the block effect at the edge of Ref. [6], but also overcomes incomplete dehazing effects and unclear details of Refs.[13] and [14] that are based on deep learning for restoration. However, the dehazing effects of our method are unstable due to the lack of a large amount of real training data on hazy days and the use of synthetic datasets.

Additionally, Fig.7 shows that the proposed algorithm dehazes the sky region more thoroughly and the restored images have clear brightness and natural colors, especially at the boundary between the sky and the mountain, owing

to the corrected compensation transmission. It not only overcomes color cast and over-saturation after dehazing by Ref. [7], but also overcomes incomplete dehazing by Refs.[13] and [14]. The algorithm in Ref.[9] solves halo and artifacts problems introduced by the minimum filtering in Ref. [6] by using a power-law compression function to obtain the dark channel map of hazy images. Although there is a slightly incomplete dehazing phenomenon, the dehazing effect is relatively good. Ref.[10] has a good dehazing effect with slightly over-saturated dehazing effect.

In Fig.8, our method has better restoration effects on the test set. In the sky regions, there are over-saturation and halo effects by Refs.[6] and [7], there are distortion, halos, darker colors, and over-saturation by Refs.[13] and [14], there are incomplete dehazing effects and unclear details by Ref.[9], and there is a slight over-saturation phenomenon by Ref.[10]. In contrast, the dehazing effects of our method are better, with the haze removed basically, the characteristics of far and near scenes maintained, and good results in details, colors, and brightness.

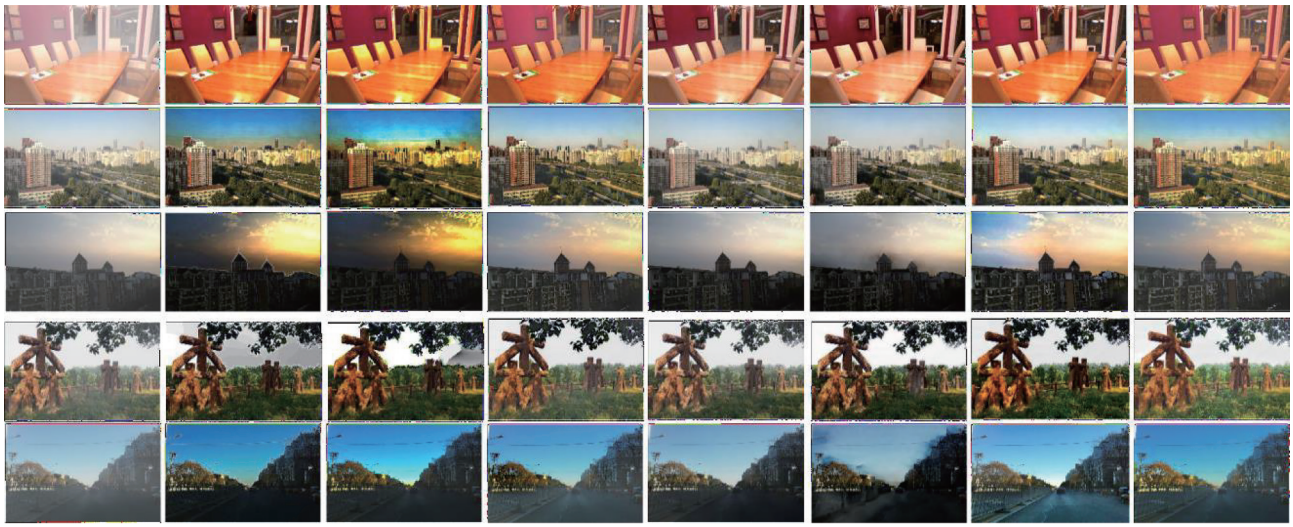

(a)Hazy image (b) Ref.[6] (c) Ref.[7] (d) Ref.[9] (e) Ref.[13] (f) Ref.[14] (g) Ref.[10] (h) Our method

**Fig. 8 Comparison of restoration results of hazy images on test set**

### 3.2 Objective evaluation

To further verify the feasibility and effectiveness of our method, we select some image quality evaluation indicators in Refs.[21-23] to objectively verify the image dehazing effects, including new visible edge rate ($e$), average gradient ($r$), information entropy ($s$), and running time ($t$). The larger the $e$, $r$, and $s$ values, the better the dehazing efffects, and the smaller the $t$, the better the dehazing efffects. Furthermore, peak signal to noise ratio (PSNR) and structural similarity (SSIM) are adopted as evaluation metrics of the images recovered from the test set, and the larger the PSNR and SSIM values, the better the dehazing effects. These metrics are calculated by

$$e=\frac{n_r-n_0}{n_0}, \tag{20}$$

$$r=\exp\left(\frac{1}{n_r}\sum_{p_i\in\varphi_r}\ln r_i\right), \tag{21}$$

$$s=-\sum_{i=1}^{L}\frac{H_w}{MN}\log_2\frac{H_w}{MN}, \tag{22}$$

where $n_0$ is the number of visible edges of the hazed image, $n_r$ is the number of visible edges of the recovered image; $r_i$ is the average gradient ratio between the recovered image and the original hazed image at $p_i$, $\varphi_r$ is the set of visible edges of the recovered image, $M$ and $N$ denote the width and height of the image respectively, $L$ is the highest grey level of the image, and $H_w$ is the number of pixels with grey level $w$.

$$R_{\mathrm{PSN}}=10\lg\frac{f_{\max}^2}{\sigma_{\mathrm{MSE}}}, \tag{23}$$

$$\sigma_{\mathrm{SSIM}}=\frac{(2\mu_i\mu_0+w_1)(2\sigma_i\sigma_0+w_2)}{(\mu_i^2+\mu_0^2+w_1)(\sigma_i^2+\sigma_0^2+w_2)}, \tag{24}$$

where $f_{\max}$ is the maximum pixel value usually taken as 255, $\sigma_{\mathrm{MSE}}$ is the mean square error of the original hazy image and the recovered image, $\sigma_{\mathrm{SSIM}}$ is the structural similarity, $R_{\mathrm{PSN}}$ is the peak signal-to-noise ratio, $\mu_i$ and $\mu_0$ are the mean values of the hazy image and the clear image respectively, $\sigma_1$ and $\sigma_2$ are the covariances of the hazy image and the clear image respectively, $w_1$ and $w_2$ are the constants to avoid the denominator being zero. In our work, objective evaluation metrics are calculated for the real hazy images in Figs.6 and 7 as well as the synthetic hazy images in the test set in Fig.8. The objective evaluation metrics of the real hazy images are

shown in Table 1.

**Table 1 Objective evaluation on indicators *e*, *r*, *s* and *t***

| Method | *e* | *r* | *s* | *t* |
|---|---|---|---|---|
| Ref.[6] | 0.203 | 1.032 | 15.899 | 1.892 |
| Ref.[7] | 0.083 | 1.187 | 15.612 | 1.624 |
| Ref.[9] | 0.216 | 1.201 | 16.019 | 0.554 |
| Ref.[13] | 0.08 | 1.107 | 15.896 | 0.336 |
| Ref.[14] | 0.011 | 1.031 | 14.991 | 0.616 |
| Ref.[10] | 0.431 | 1.109 | 16.001 | 1.418 |
| Our method | 0.475 | 1.236 | 16.203 | 1.662 |

It can be seen that the proposed algorithm achieves better results in terms of new visible edges, average gradient, information entropy and running time, especially in terms of new visible edges and information entropy metrics.

In Table 2, the PSNR and SSIM of the recovered images on the test set of our method are not as good as those of Ref. [13], which has the highest PSNR and SSIM. However, in combination with the subjective results, the recovery results of Ref. [13] are found to have too much haze residue and poor visual effects. This is due to an overfitting problem during the training of its network. This also shows that a single metric comparison does not fully illustrate the strength and weakness of the algorithm. In a word, as for the recovery of real hazy images and the recovery of images on the test set, our method achieves good results. Combining subjective and objective evaluation metrics, it can be seen that our method performs well in all these performance metrics. Therefore, its feasibility and effectiveness are proven.

**Table 2 Indicators on different datasets**

| Method | PSNR | SSIM |
|---|---|---|
| Ref.[6] | 16.001 | 0.868 |
| Ref.[7] | 16.821 | 0.830 |
| Ref.[9] | 17.682 | 0.817 |
| Ref.[13] | 25.596 | 0.946 |
| Ref.[14] | 18.840 | 0.903 |
| Ref.[10] | 21.010 | 0.850 |
| Our method | 20.896 | 0.931 |

## 4 Conclusions

In order to address problems of halos, artifacts and incomplete dehazing in hazy sky image clarification processing, we propose a dehazing algorithm based on negative haze concentration correction to compensate for transmission. DCP is not good at dealing with sky and edge regions, so an error mechanism is proposed to compensate for the transmission, and then haze concentration is constructed based on the grey scale co-generation matrix combined with differential curvature to adaptively correct the compensated transmission to obtain accurate transmission. Local atmospheric light is then improved using channel difference fusion in the channel. Finally, the haze-free image is recovered from the atmospheric scattering model. Experimental results demonstrate that our method can suppress halo, artifacts and dehaze incompleteness very well.

## Acknowledgement

This work was supported by College Industry Support Plan Project of Gansu Provincial Department of Education (No.2021CYZC-04).

## Declaration of conflicting interests

The authors have no conflict of interests related to this publication.

## References

[1] WANG D L, ZHANG T Y. Review and analysis of image defogging algorithm. Journal of Graphics, 2020, 41(6): 861-870.

[2] KIM J H, JANG W D, SIM J Y, et al. Optimized contrast enhancement for real-time image and video dehazing. Journal of Visual Communication and Image Representation, 2013, 24(3): 410-425.

[3] HAN J W, ZHANG D W, CHANG G, et al. Object detection in optical remote sensing images based on weakly supervised learning and high-level feature learning. IEEE Transactions on Geoscience Remote Sensing, 2015, 53(6): 3325-3337.

[4] LIU H B, YANG J, WU Z P. A fast single image fog method based on dark channel prior and Retinex theory. Journal of Automation, 2015, 41(7): 1264-1273.

[5] ZHANG H, LIU X, HUANG Z T, et al. Single image dehazing based on fast wavelet transform with weighted image fusion//2014 IEEE International Conference on Image Processing, October 27-30, 2014, Paris, France. New York: IEEE, 2015: 4542-4546.

[6] HE K M, SUN J, TANG X O. Single image haze removal using dark channel prior//2009 IEEE Conference on Computer Vision and Pattern Recognition, June 20-25, 2009, Miami, FL, USA. New York: IEEE, 2009: 1956-1963.

[7] AGRAWAL S C, JALAL A S. Dense haze removal by nonlinear transformation. IEEE Transactions on Circuits and Systems for Video Technology, 2022, 32(2): 593-607.

[8] ZHU Q S, MAI J M, SHAO L. A fast single image haze removal algorithm using color attenuation prior. IEEE Transactions on Image Processing, 2015, 24(11): 3522-3533.

[9] YANG Y, WANG Z W. Haze removal: push DCP at the edge. IEEE Signal Processing Letters, 2020, 27: 1405-1409.

[10] YANG Y, ZHANG J L, LIU C, et al. Visibility restoration of haze and dust image using color correction and composite

channel prior. The Visual Computer: International Journal of Computer Graphics, 2022, 39(7): 2795-2809.
[11] REN W Q, MA L, ZHANG J W, et al. Gated fusion network for single image dehazing//2018 IEEE/CVF Conference on Computer Vision and Pattern Recognition, June 18-23, 2018, Salt Lake City, UT, USA. New York: IEEE, 2018: 3253-3261.
[12] LI B Y, PENG X L, WANG Z Y, et al. AOD-net: all-in-one dehazing network//2017 IEEE International Conference on Computer Vision, October 22-29, 2017, Venice, Italy. New York: IEEE, 2017: 4780-4788.
[13] QIN X, WANG Z L, BAI Y C, et al. FFA-Net: feature fusion attention network for single image dehazing. Proceedings of the AAAI Conference on Artificial Intelligence, 2020, 34(7): 11908-11915.
[14] BAI H R, PAN J S, XIANG X G, et al. Self-guided image dehazing using progressive feature fusion. IEEE Transactions on Image Processing, 2022, 31: 1217-1229.
[15] YANG Y, WANG Z W. Image restoration algorithm based on compensated transmission and adaptive haze concentration coefficient. Journal on Communications, 2020, 41(1): 66-75.
[16] JU M Y, ZHANG D Y, JI Y T. Image defogging algorithm based on fog concentration estimation. Journal of Automation, 2016, 42(9): 1367-1379.
[17] YUAN S, CHEN Y Y, SHI H. An image defogging algorithm based on a priori improvement of fog line dark channel. Advances in Lasers and Optoelectronics, 2022, 59(8): 181-188.
[18] SUN W, WANG H, SUN C H, et al. Fast single image haze removal *via* local atmospheric light veil estimation. Computers & Electrical Engineering, 2015, 46: 371-383.
[19] YANG Y, QIU G Y, HUANG S Y, et al. A single image defogging method based on improved atmospheric scattering model. Journal of Beijing University of Aeronautics and Astronautics, 2022, 48(8): 1364-1375.
[20] SUN J R, XIE L C, DU M X, et al. A nonlinear transformed adaptive transmission defogging algorithm. Journal of Xi′an University of Electronic Science and Technology, 2022, 49(1): 208-215.
[21] CHOI L K, YOU J, BOVIK A C. Referenceless prediction of perceptual fog density and perceptual image defogging. IEEE Transactions on Image Processing, 2015, 24(11): 3888-3901.
[22] MIN X K, ZHAI G T, GU K, et al. Objective quality evaluation of dehazed images. IEEE Transactions on Intelligent Transportation Systems, 2019, 20(8): 2879-2892.
[23] HAN H N, QIAN F, LU J W, et al. Quality evaluation of image defogging methods. Optical Precision Engineering, 2022, 30(6): 721-733.

# 基于负向雾浓度矫正的透射率补偿去雾算法

吕东霞, 杨 燕

兰州交通大学 电子与信息工程学院, 甘肃 兰州 730070

**摘 要:** 针对雾天图像清晰化处理存在光晕、伪影、去雾不彻底等问题, 提出一种基于负向雾浓度矫正补偿透射率的去雾算法。首先, 利用误差机制对暗通道透射率进行补偿。其次, 分析透射率、景深和雾浓度的关系, 构造负向雾浓度模型对透射率进行自适应伽马矫正。最后, 提出通道差异融合中通道修正大气光, 结合大气散射模型恢复无雾图像。实验结果表明, 所提出的算法解决了光晕、伪影、去雾不彻底等问题且恢复的图像细节突出、亮度适宜、色彩自然。

**关键词:** 图像去雾; 补偿透射率; 负向雾浓度; 通道差异; 局部大气光

**引用格式:** LÜ Dongxia, YANG Yan. A dehazing algorithm of compensated transmission based on negative haze concentration correction. Journal of Measurement Science and Instrumentation, 2026, 17(1): 88-96. DOI: 10.62756/jmsi.1674-8042.2026007